J. Braz. Chem. Soc., Vol. 21, No. 11, 2155-2163, 2010.
Printed in Brazil - ©2010 Sociedade Brasileira de Química
0103 - 5053 $6.00+0.00

Article

2-Chlorovinyl Tellurium Dihalides, (*p*-tol)Te[C(H)=C(C*l*)Ph]X_2 for X = C*l*, Br and I: Variable Coordination Environments, Supramolecular Structures and Docking Studies in Cathepsin B

Ignez Caracelli,*,[a] Julio Zukerman-Schpector,*,[b] Stella H. Maganhi,[b] Hélio A. Stefani,[c] Rafael Guadagnin[d] and Edward R. T. Tiekink*,[e]

[a]*Departamento de Física, Universidade Federal de São Carlos, CP 676, 13565-905 São Carlos-SP, Brazil*

[b]*Laboratório de Cristalografia, Estereodinâmica e Modelagem Molecular, Departamento de Química, Universidade Federal de São Carlos, CP 676, 13565-905 São Carlos-SP, Brazil*

[c]*Departamento de Farmácia, Faculdade de Ciências Farmacêuticas, Universidade de São Paulo, São Paulo-SP, Brazil*

[d]*Departamento de Química, Universidade Federal de São Paulo, São Paulo-SP, Brazil*

[e]*Department of Chemistry, University of Malaya, 50603 Kuala Lumpur, Malaysia*

Os estudos cristalográficos mostram que o poliedro de coordenação ao redor do átomo de Te, em cada um dos compostos (*p*-tol)Te[C(H)=C(C*l*)Ph]X_2, com X = C*l* (**1**), Br (**2**) e I (**3**), é uma Ψ-bipirâmide pentagonal distorcida. O grupo vinil em (**1**) adota uma configuração *E* o que impede a formação de uma interação intramolecular Te···C*l* e em seu lugar é encontrada uma interação intramolecular Te···π. O poliedro de coordenação é formado por um arranjo linear C*l*–Te–C*l* com o plano pentagonal definido por dois átomos de C dos substituintes orgânicos, um contato intermolecular Te···C*l*, uma interação Te···π e um par isolado de elétrons estereoquimicamente ativo. Geometrias de coordenação semelhantes são encontradas para as estruturas com X = Br (**2**) e I (**3**), mas a interação π é substituída por uma interação intramolecular Te···C*l* devido à adoção de uma configuração *Z* em torno da ligação vinil. As diferenças nas estruturas são facilmente explicadas em termos de efeitos eletrônicos. Estudos de docking em catepsina B com (**1'**)-(**3'**), ou seja, compostos **1** a **3** em que há um haleto a menos ligado ao átomo de Te, mostram que há uma ligação eficiente com a proteína pela formação da ligação covalente Te–S_{Cys29} com a estabilização proporcionada por uma combinação de interações N–H···π, C–H···π e Cl_{vinyl}···H. Estes resultados são comparáveis aos obtidos com inibidores conhecidos da catepsina B o que sugere que os compostos estudados têm potencial atividade biológica.

Crystallography shows that the Te atom in each of (*p*-tol)Te[C(H)=C(C*l*)Ph]X_2, for X = C*l* (**1**), Br (**2**) and I (**3**), is within a distorted Ψ-pentagonal bipyramidal geometry. An *E* configuration for the vinyl group in (**1**) precludes the formation of an intramolecular Te···C*l* interaction so that an intramolecular Te···π interaction is found instead. The coordination environment features a linear C*l*–Te–C*l* arrangement with the pentagonal plane defined by the two C atoms of the organic substituents, an intermolecular Te···C*l* contact, a Te···π interaction and a stereochemically active lone pair of electrons. In the X = Br (**2**) and I (**3**) structures, similar coordination geometries are found but the Te···π contact is replaced by an intramolecular Te···C*l* contact owing to the adoption of a Z configuration about the vinyl bond. The differences in structure are readily explained in terms of electronic effects. Docking studies of cathepsin B with (**1'**)-(**3'**), *i.e.* **1**-**3** less one Te–bound halide, show efficient binding through the agency of covalent Te–S_{Cys29} bonds with stabilization afforded by a combination of N–H···π, C–H···π and Cl_{vinyl}···H interactions. These results comparable favorably with known inhibitors of cathepsin B suggesting the title compounds have potential biological activity.

Keywords: organotellurium-dihalides, docking studies, cathepsin B, crystal structures, supramolecular arrangements

*e-mail: ignez@ufscar.br, julio@power.ufscar.br, edward.tiekink@gmail.com

Introduction

Organotellurium halides comprise an interesting class of compounds owing to the great diversity displayed in their molecular and supramolecular arrangements, as well as for their biological activity. It is observed that in most cases the geometry around the Te atom is governed by the presence of secondary bonds, which may be intra- or inter-molecular in origin, and which give rise to a wide variety of coordination polyhedra as well as supramolecular assemblies.[1-5] With reference to the biological activity of Te(IV) compounds, in 1987 Sredni *et al*.[6] reported the immunomodulating properties of ammonium trichloro(dioxyethylene-*O*,*O*') tellurate (AS101). This was followed in 1998, by the observation by Albeck *et al.*[7] that some organotellurium compounds were cathepsin B inhibitors. In particular, the irreversible inhibition activity of AS101 was described and, subsequently, an extensive study of other biological properties of this compound ensued.[8-11] As cathepsin B is involved in a number of human diseases,[12-14] the development of selective inhibitors of cathepsin B has become a mainstay in the search of chemotherapeutic agents.[15] Recently, Cunha *et al.*[16,17] presented a series of eight organotellurium(IV) compounds which exhibited more effective inhibition of Cathepsin B compared with AS101. Moreover, in order to gain greater insight of the inhibition mechanism, a docking study was undertaken providing some clues as to why organic telluranes are more efficient inhibitors than their inorganic counterparts, such as AS101. [18]

In continuation of our on-going interest in Te(IV) compounds,[1-3,5,18] we report here the synthesis, molecular and supramolecular arrangements of three dihalo-organotellurium compounds (Scheme 1). In order to assess the possibility of using these compounds as cathepsin B inhibitors, docking studies at the active site of cathepsin B were also performed, and, for comparison, investigations were performed for dichloro-((*Z*)-2-chloro-phenylvinyl)-4-methoxyphenyl-tellurium(IV), (**4**) (CSD code YOWMEC),[19] which is a proven cathepsin B inhibitor.[16]

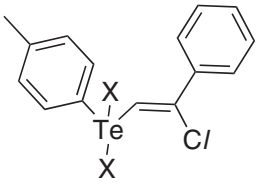

X = **1** C*l*, **2** Br, **3** I

Scheme 1.

Experimental

Synthesis

The trichloride compound was prepared through the addition reaction of (*p*-tolyl)tellurium trichloride to phenyl acetylene to produce the 2-chlorovinyl tellurium dichloride. Compounds containing bromide and iodine atoms were prepared from the trichloride using bromine, and iodine as halide sources, respectively (Scheme 2).[20]

Crystal structure determination

The crystal structures were solved by direct methods.[21] Full-matrix least-squares refinement (on F^2)[22] with anisotropic displacement parameters for all non-hydrogen atoms was performed. The H atoms were placed on stereochemical grounds and refined with fixed geometry, each riding on a carrier atom with an isotropic displacement parameter amounting to 1.2 times (1.5 for methyl–H) the value of the equivalent isotropic displacement parameter of the carrier atom to which the H atom is attached. The

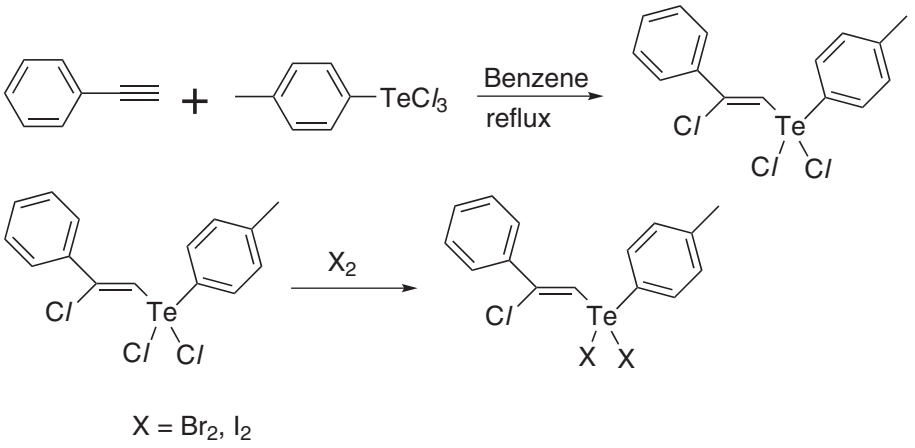

Scheme 2.

programs PARST95,[23] PLATON,[24] WinGX,[25] ORTEP3 for Windows,[26] MarvinSketch 5.1.10[27] and DIAMOND[28] were used for geometrical calculations and to prepare crystallographic material for publication.

Docking studies

Docking studies were performed with the GOLD program (version 4.1.1), which uses a genetic algorithm to explore the full range of ligand conformational flexibility with partial flexibility of the protein binding site.[29] The GOLDScore function which uses bond strengths in the fitness function and has the form:

$$f = S_{hb\_ext} + S_{vdw\_ext} + S_{hb\_int} + S_{vdw\_int}$$

where S_{hb_ext} is the protein-ligand hydrogen bonding score, and S_{hb_int} the internal hydrogen bonding of the ligand. Usually, the best result is obtained by allowing the internal hydrogen bonding tend to zero, and S_{vdw_ext} and S_{vdw_int}, *i.e*. the scores arising from weak van der Waals forces,[30] set to select the best ligand-cathepsin B complex at each of 10 independent genetic algorithm runs *per* ligand. At each run 100,000 genetic operations were carried out (*ca*. 47,250 mutations, *ca*. 47,250 crosslinkings and *ca*. 5,000 migrations).

The 1gmy structure of cathepsin B was selected and retrieved from the Protein Data Bank (PDB) and PDBSum.[31,32] The hydrogen atoms were added using the facilities within GOLD, and all water molecules and hetero atoms were removed from the protein. As it was postulated that the irreversible inhibition of cathepsin B by organotellurium(IV) compounds is due to the high nucleophilic character of the thiol–S at the active site combined with the electrophilic character of the Te atom,[16,17] the Cys29 and the His199 residues, within the active site, were set in the ionized forms. As has already been described, the His110 and His111 were protonated at their imidazole-N atoms.[18] The docking calculations were performed using a 12 Å sphere around the Cys29–S atom allowing rotamers for Cys29, His199 and Tyr75, and full flexibility of the organotellurium(IV) compounds, hereafter referred to as ligands. The GOLD program parameters were validated by performing the re-docking of the known inhibitor *N*-cyanomethyl-*N*α-(diphenylacetyl)-3-methylphenyl-alaninamide, as demonstrated by crystallographic studies.[31]

Docking simulations were performed in three steps. First, calculations were conducted with the complete ligand molecule which resulted in an approximate Te···S_{Cys29} distance of *ca*. 6 Å (Table S1, Supplementary Information, SI), obviously a distance that precludes the formation of a covalent bond. As mentioned earlier, it is known that these kinds of molecules are irreversible inhibitors of cathepsin B,[16-18] an observation inevitably due to the formation of a Te–S_{Cys29} bond. In order to allow the formation of a covalent bond between the Te and S_{Cys29} atoms, one of tellurium-bound halide atom was removed prior to calculating the interaction with cathepsin B; in these calculations, the Te–S_{Cys29} distance was constrained to be in the range 2.0-3.3 Å. As shown from crystallography (see below), the tellurium-bound halogen atoms are non-equivalent, so the calculations were performed with either halide removed. The calculations showed that the most efficient interactions were obtained for the ligand in which the halide furthest away from the Te-bound phenyl group was removed. The evaluation and selection of the complexes constructed in the docking calculations was accomplished by combining graphic analyses[33] of the favorable interactions and numerical comparison of the GOLDScore values. Equivalent complexes were grouped and those with best scores selected. The binding mode selected was that with the highest score and a favorable orientation in the active site.

Results and Discussion

Crystallographic structures

Details of unit cell data, X-ray data collection, structure solution and refinement for (**1**)-(**3**) are given in Table 1. A complete list of atomic coordinates, bond distances and angles, anisotropic displacement parameters, and hydrogen atom coordinates have been deposited, and are available upon request (see footnote to Table 1).

The molecular structure of (*p*-tol)Te[C(H)=C(C*l*)Ph]-Cl_2 (**1**) is illustrated in Figure 1(a) and salient geometric parameters are collected in Table 2. The immediate coordination environment of the Te atom is tetra-coordinated defined by two C*l* atoms as well as two C atoms, derived from the two organic substituents. The Te–C_{vinyl} bond distance of 2.104(3) Å is significantly shorter than the Te–C_{tolyl} distance of 2.137(3) Å, consistent with the vinyl group being more electron rich thereby forming the stronger bond. The configuration about the C1=C2 bond [1.322(4) Å] is *E* meaning the C*l*3 atom is directed away from the Te centre precluding an intramolecular Te···C*l*3 interaction. However, a close intermolecular Te···C*l*2^{i} interaction, Table 2, is observed; symmetry operation *i*: 2-*x*, 1-*y*, 1-*z*. In addition, the Te···ring centroid(C3-C8) distance of 4.10 Å, while at the extreme end of Te···π distances,[3] must be considered a significant interaction as the ring clearly occupies a coordination site (see below). The final

Table 1. Crystallographic data and refinement details[a]

Compound	**1**	**2**	**3**
Formula	$C_{15}H_{13}Cl_3Te$	$C_{15}H_{13}Br_2ClTe$	$C_{15}H_{13}ClI_2Te$
Formula weight	427.20	516.12	610.10
Crystal system	Monoclinic	Triclinic	Triclinic
Space group	$P2_1/c$	$P\bar{1}$	$P\bar{1}$
a (Å)	11.900(2)	7.6299(18)	8.3253(19)
b (Å)	9.7334(14)	8.6899(19)	8.904(2)
c (Å)	14.625(2)	12.766(3)	12.601(3)
α (º)	90	91.785(3)	94.514(4)
β (º)	112.940(3)	93.890(4)	93.162(2)
γ (º)	90	104.868(5)	109.399(4)
V (Å^3)	1560.1(4)	815.2(3)	875.0(3)
D_c (g cm^{-3})	1.819	2.103	2.316
Z	4	2	2
μ(MoKα) (mm^{-1})	2.404	6.874	5.367
F(000)	824	484	556
Crystal size (mm)	0.06 × 0.20 × 0.20	0.10 × 0.15 × 0.20	0.10 × 0.18 × 0.30
θ range for data collection (º)	2.6 to 27.5	2.8 to 27.5	2.8 to 27.5
Reflections collected	6179	6240	6060
Independent/observed refls. [$I > 2\sigma(I)$]	3563 / 3334 (R_{int} = 0.019)	3712 / 3480 (R_{int} = 0.025)	3982 / 3833 (R_{int} = 0.036)
No. of parameters	173	173	174
GOF on F^2	1.10	1.09	1.16
a, *b* in weighting scheme	0.021 / 1.924	0.031 / 1.332	0.058 / 2.331
Final *R* indices (obs. data)	*R*1 = 0.027, *wR*2 = 0.056	*R*1 = 0.037, *wR*2 = 0.075	*R*1 = 0.041, *wR*2 = 0.110
R indices (all data)	*R*1 = 0.029, *wR*2 = 0.058	*R*1 = 0.034, *wR*2 = 0.076	*R*1 = 0.042 *wR*2 = 0.111
Largest diff. peak and hole (e Å^{-3})	0.86 and –0.53	0.89 and –0.75	1.29 and –1.20

[a]Crystallographic data (excluding structure factors) for the structures reported in this paper have been deposited with the Cambridge Crystallographic Data Centre as supplementary publications no. CCDC- 673979, 673980, 673981. Copies of available material can be obtained free of charge, on application to CCDC, 12 Union Road, Cambridge CB2 1EZ, UK, (fax: +44-(0)1223-336033 or e-mail: deposit@chemcrys.cam.ac.uk). The list of Fo/Fc-data is available from the author up to one year after the publication has appeared.

position in the coordination geometry of the Te^{IV} center is occupied by a stereochemically active lone pair of electrons that is located in the region between the Te···C*l*2^i and Te···π interactions. While lone pair···π and metal···π interactions are not often observed, they are increasingly being recognized as being important in determining coordination geometries and as supramolecular synthons when other intermolecular interactions are not present.[3-5,34-36] In the present case, the Te···π interaction must be considered as donation of electron density from the aromatic ring to Te. Overall, the coordination geometry is best described as distorted Ψ-pentagonal bipyramidal with the covalently bound C*l* atoms defining the axial positions [C*l*1-Te-C*l*2 = 173.57(2)º]. The presence of the intermolecular Te···C*l*2^i readily explains the significant elongation of the Te-C*l*2 bond distance [2.5516(7) Å] compared with the Te-C*l*1 bond [2.4719(7) Å].

There are three closely related structures available for comparison with (**1**), namely PhTe[C(H)=C(C*l*)Ph]Cl_2[37] and (*p*-MeOPh)Te[C(H)=C(C*l*)Ph]Cl_2,[19] *i.e.* with the same vinyl group but with different aryl groups, and (*p*-MeOPh)Te[C(H)=C(C*l*)PhMe-*p*]Cl_2,[38] *i.e.*, where both organic substituents differ from those in (**1**). Selected geometric parameters for these structures are also collected in Table 2. The most notable difference between the molecular structures of these and that of (**1**) is found in the relative orientation of the vinyl-bound C*l* atom whereby the configuration about the vinyl C=C bond is *Z* in direct contrast to the *E* configuration observed in (**1**). This orientation allows for the formation of intramolecular Te···C*l* interactions. Each of the three literature structures features a distorted Ψ-pentagonal bipyramidal geometry with *trans* C*l* atoms, and with the approximate pentagonal plane defined by two C atoms,

Table 2. Selected bond distances, in Å, and angles (°)

Compound	Te–C*l*1	Te–C*l*2	C*l*1–Te–C*l*2	Te–C_{vinyl}	C1–C2	Te···C*l*3	Te···C*l*[a]	Te···π	Ref.
(**1**)	2.4719(7)	2.5516(7)	173.57(2)	2.104(3)	1.322(4)	(*E*)	3.361(3)	4.10 (intra)	
YOWMEC (**4**)	2.521(3)	2.485(3)	177.66(11)	2.074(8)	1.3449(11)	3.263(3)	3.658(3)	4.06	19[a]
GOKFAO	2.5202(8)	2.5027(8)	177.22(2)	2.128(2)	1.325(4)	3.2593(8)	3.3767(8)	4.37	37
GOKDUG	2.5016(7)	2.5108(7)	171.73(2)	2.079(2)	1.335(3)	3.2510(8)	3.7363(9)	–	37
JILXAD	2.522(3)	2.478(3)	177.65(10)	2.086(6)	1.325(9)	3.280(3)	3.732(2)	4.01	38
ASEHUB	2.487(3)	2.529(3)	175.20(7)	2.128(6)	1.300(9)	(*E*) 2.722(5)	–	–	40
ASEHUB01	2.5056(16)	2.5315(16)	175.27(8)	2.122(4)	1.308(5)	(*E*) 2.704(3)	3.8373(19)	–	40
HABHIC[a]	2.505(2)	2.518(2)	175.28(8)	2.086(6) [2.097(6)]	1.317(8) [1.306(8)]	3.290(3) [3.253(2)]	–	3.76	41
QOGPAD	2.4918(12)	2.5160(12)	171.45(4)	2.077(4)	1.311(5)	3.2095(14)	3.6364(13)		42
YUFNUI	2.532(4)	2.473(4)	176.90(12)	2.094(12)	1.341(19)	3.283(4)	3.681(4)	4.00	43
	Te–Br1	Te–Br2	Br1–Te–Br2				Te···Br		
(**2**)	2.6397(5)	2.7213(5)	178.505(13)	2.098(3)	1.332(5)	3.352(1)	3.479(1)	–	
CIDGIF01	2.625(3)	2.732(3)	171.10(9)	2.076(9)	1.333(12)	3.2541(18)(Br3)	4.330(9)	–	44
SEFKAP	2.6114(10)	2.7296(10)	176.59(3)	2.092(7)	1.308(9)	3.4879(10)(Br3)	3.041(6) (O1)	–	45
XUCNIS	2.6402(15)	2.7184(15)	176.50(4)	2.096(9)	1.325(11)	(*E*)	4.035(2) (Br1)	–	46
XUCNOY	2.632(3)	2.715(3)	175.22(8)	2.111(16)	1.32(2)	3.354(2) (Br3)	3.606(2) (Br2)	–	46
XAGVIK	2.5766(13)	2.6591(12)	169.90(4)	2.134(7)	1.273(11)	(*E*)	3.5774(12) (Br1)	–	
	Te–I1	Te–I2	I1–Te–I2						
(**3**)	2.8731(6)	2.9670(6)	177.618(12)	2.103(5)	1.328(7)	3.322(2) (C*l*)	3.677(1) (I2)	–	

[a][PhC(C*l*)=(H)C]Te[C(H)=C(C*l*)Ph]$C*l*_2$. (*E*) = entgegen

two loosely associated C*l* atoms, and the stereochemically active lone pair of electrons. The relationship between the structure of (**1**) and the literature structures is simple in that the intramolecular Te···π interaction observed in (**1**) has been replaced by an intramolecular Te···C*l* interaction in each case. The question then arises, why are the Te···C*l* interactions in the literature structures usurped by a Te···π interaction in (**1**). The answer is electronic in origin and is based on a literature precedent of a systematic evaluation of phosphinegold(I) thiolates containing phenyl- and isomeric tolyl-phosphine ligands and similarly substituted thiolates.[39] Comparing the three structures with the same vinyl group, it is noted that the aryl ring, *i.e., p*-tolyl, in **1** is activated compared to both *p*-MeOPh and Ph aryl groups in (*p*-MeOPh)Te[C(H)=C(C*l*)Ph]$C*l*_2$,[19] and PhTe[C(H)=C(C*l*)Ph]$C*l*_2$,[37] respectively. Such activation imparts *relatively* more electron density to the Te atom, making it less Lewis acidic allowing for the formation of a presumably weaker Te···π interaction *in lieu* of the putative intramolecular Te···C*l* interaction. Next, attention is directed to an evaluation of the molecular structures of the di-bromo and di-iodo analogues of (**1**), *i.e.*, (*p*-tol)-Te[C(H)=C(C*l*)Ph]Br_2 (**2**) and (*p*-tol)Te[C(H)=C(C*l*)Ph]-I_2 (**3**), respectively, having less electronegative halides bound to Te compared to C*l* in (**1**).

The molecular structures of isomorphous **2** and **3** are illustrated in Figures 1(b) and (c), respectively, and immediately apparent from these is that the vinyl ligand adopts the *Z* configuration in contrast to that observed for **1**; selected geometric parameters are collated in Table 2. The isomerism in the vinyl ligand allows for the formation of intramolecular Te···C*l*3 interactions, an observation that correlates nicely with the decreased Lewis acidity of the Te atom in each of **2** and **3**, owing to the presence of the less electronegative Br and I atoms, respectively, compared to that in **1**, with electronegative C*l* atoms. The distorted Ψ-pentagonal bipyramidal coordination geometry in each of **2** and **3** is defined by two axially coordinated halides, with the two C atoms, two weakly associated C*l* atoms, and the stereochemically active lone pair of electrons defining the pentagonal plane.

Whereas the majority of structures conforming to the general molecular formula RTe[C(H)=C(X)R']X_2 adopt the *Z* configuration allowing for the formation of an intramolecular Te···X interaction,[19,37-40,41-46] some exceptions are noted; disordered structures are not included in the compilation given in Table 2. As indicated in Table 2, several structures feature intramolecular Te···O interactions, where the O atom is derived from a proximate hydroxyl substituent, in preference to the Te···C*l* contact.

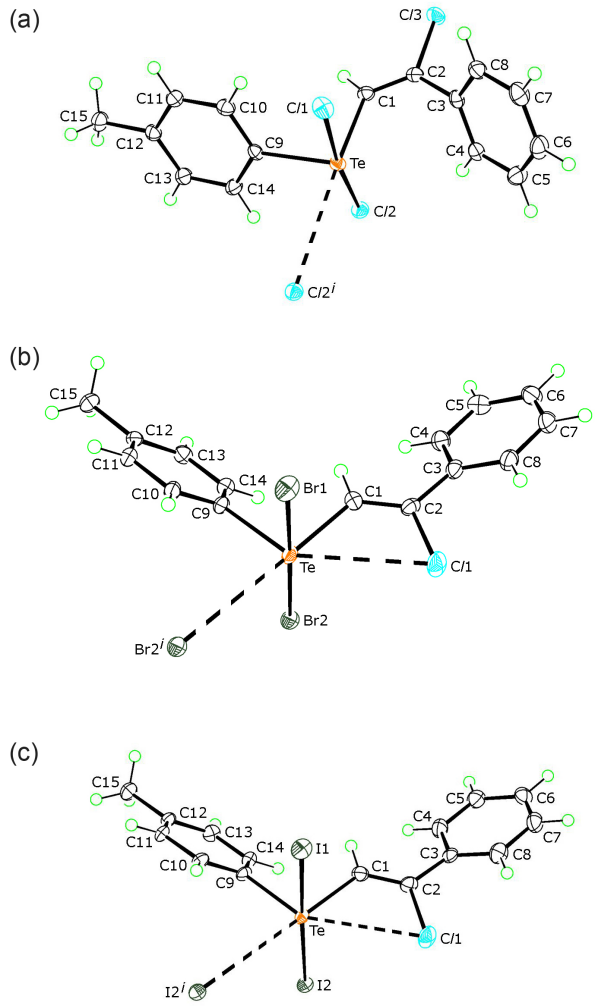

Figure 1. Molecular structures of (a) (*p*-tol)Te[C(H)=C(C*l*)Ph]$C*l*_2$ (**1**), showing the intermolecular Te···C*l*2^i contact as a dashed line; symmetry operation *i*: 2-*x*, 1-*y*, 1-*z*; (b) (*p*-tol)Te[C(H)=C(C*l*)Ph]Br_2 (**2**); and (c) (*p*-tol)Te[C(H)=C(C*l*)Ph]I_2 (**3**). For (b) and (c), the intramolecular Te···C*l*1 and intermolecular Te···C*l*2^i contacts are shown as dashed lines; symmetry operation *i*: -*x*, 1-*y*, -*z*.

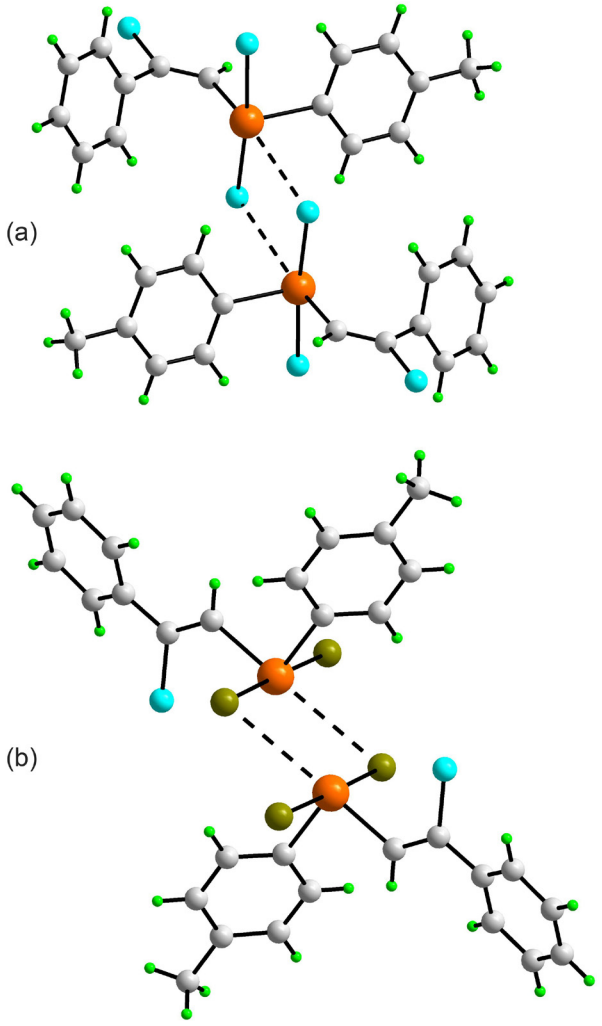

Figure 2. Supramolecular aggregation via Te···X interactions between centrosymmetrically related molecules in (a) (*p*-tol)Te[C(H)=C(C*l*)Ph]$C*l*_2$ (**1**), X = C*l*; and (b) (*p*-tol)Te[C(H)=C(C*l*)Ph]X_2 (**2**) and (**3**), illustrated for X = Br. For reasons of clarity, the intramolecular Te···X contacts are not included.

Also noteworthy is the pseudo-polymorphic system PhTe[C(H)=C(Br)R']Br_2. Here, the generally adopted *Z* configuration is found to the methanol monohydrate. By contrast, the unsolvated form features an *E* configuration. Such observations emphasize the weak nature of the secondary interactions and show the importance of global crystal packing considerations upon the final molecular structure adopted in the solid state.[47]

The most prominent intermolecular interactions occurring in the crystal structures of **1**-**3** are the intermolecular Te···X interactions described above. In **1**, these lead to centrosymmetric dimers, Figure 2(a), with the vinyl-bound C*l* atoms directed away from the centrosymmetric $[TeC*l*_2]_2$ rhombus. In the isomorphous crystal structures of **2**, Figure 2(b), and **3**, centrosymmetrically related molecules also associate via Te···X interactions to form loosely associated dimers but, in these cases, the vinyl-bound C*l* atoms are directed towards the $[TeX_2]_2$ rhombus.

Docking in cathepsin B

According to Schechter and Berger's nomenclature,[48] the active site of proteases is composed of several sub-sites: those on the N-terminal side are named S1, S2, S3 … Sn, and sub-sites on the C-terminal side are named S1', S2', S3'… Sn'. Studies have shown that the inhibitory activity is dependent on binding modes and that the simultaneous binding to the S1' and S2' sub-sites leads to high inhibitory activity.[49]

The results of the docking simulations are summarized in Table 3 and Figure 3. From the GOLDScore values,

and from the similar binding patterns observed, it can be postulated that each of (**1'**)-(**4'**), *i.e.*, cations corresponding to **1**-**4** but each with a Te-bound halogen missing (see Experimental), can bind efficiently into the active site of cathepsin B, hereafter CatB. Figure 3 provides a general picture of the binding mode and the overlap of the poses, and clearly shows that four sub-sites, namely S1, S2, S1' and S2', are engaged in complex formation.

Table 3. Docking scores (kcal mol^{-1}) and $\Delta G_{binding}$ (kcal mol^{-1})

Compound	GOLDScore	$\Delta G_{binding}$
(**1'**)	45.55	–7.16
(**2'**)	43.09	–6.90
(**3'**)	44.97	–7.10
(**4'**)	42.79	–6.87

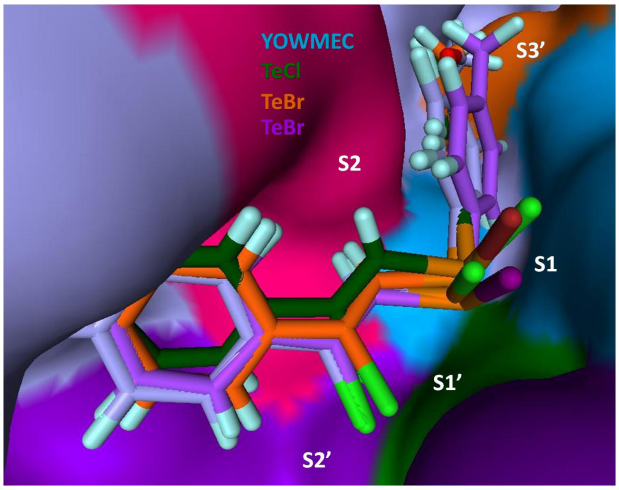

Figure 3. The four molecules docked into the active site of cathepsin B. The C atoms are shown in green for (**1'**), in orange for (**2'**), in purple for (**3'**) and in light blue for (**4'**). The subsites are colored: S1 (blue), S2 (pink), S1' (green) and S2' (violet). See the online version for colors.

In all cases, the Te-bound phenyl ring forms two π interactions, on one side via an interaction of the type N–H···π involving the Gly74 residue of S1, and on the other side via a C–H···π interaction with His199 of S2, as illustrated in Figure 4 for (**3'**). The phenyl ring attached to the vinyl moiety also participates in a C–H···π interaction, *i.e.*, with His199 of S2 as illustrated in Figure 4 for (**3'**).

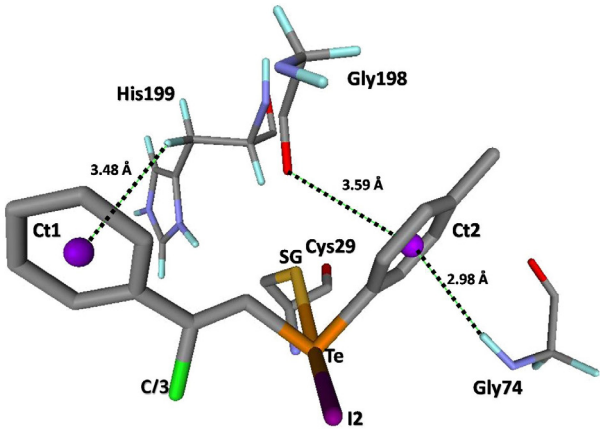

Figure 4. The interactions involving the π-systems in the docked complex with (**3'**).

The Cl_{vinyl} atom is involved in hydrogen bonding interactions with Gly27 (S1') and Gln23 (S2'), as depicted in Figure 5 for (**3'**), with geometric parameters collected in Table 4 for all four complexes.

The Cl_{vinyl} and O_{Gly27} atoms are involved in secondary intra- and inter- molecular interactions with the Te atom, respectively, so that the coordination geometry is that of a distorted Ψ-pentagonal bipyramidal, with the halogen and the S_{Cys29} atom in the apical positions; the equatorial positions are occupied by two C atoms, the Cl_{vinyl}, the

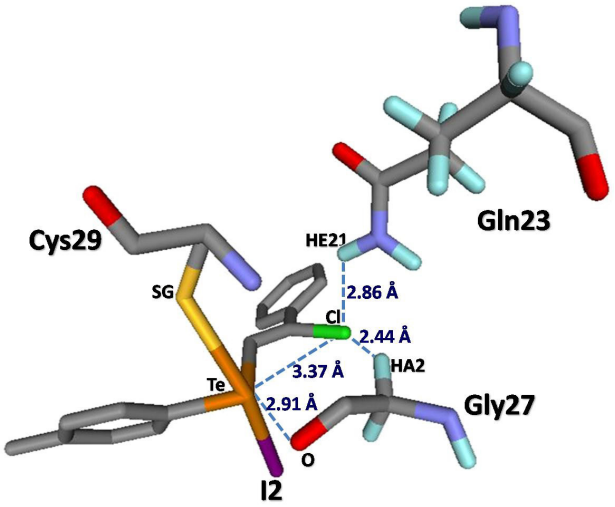

Figure 5. The coordination around the Te atom and the C-H···Cl_{vinyl} interactions for compound (**3'**).

Table 4. Geometric parameters of the H···Cl_{vinyl} interactions

Compound	Gln23 Interactions			Gly27 Interactions		
	H···Cl (Å)	N···Cl_{vinyl} (Å)	N–H···Cl_{vinyl} (°)	HA2···Cl_{vinyl} (Å)	C···Cl_{vinyl} (Å)	C–H···Cl_{vinyl} (°)
(**1'**)	2.66	3.574	151	2.91	3.718	134
(**2'**)	3.39	4.109	130	2.48	3.133	131
(**3'**)	2.86	3.559	129	2.44	3.293	118
YOWMEC	2.93	3.646	129	2.57	3.406	134

O_{Gly27}, and the stereochemically active lone pair of electrons (in the region bisecting the Te-C_{aryl} and Te···O vectors), as shown in Figure 5 for (**3'**). This result shows that the configuration about the vinyl C=C bond in the structure of (**1'**) in the docked complex, *i.e.*, *Z* is in direct contrast to the *E* configuration observed in the crystallographically determined structure. A calculation was performed whereby the crystallographically observed conformation for the ligand was retained. A significantly worse GOLDscore (*i.e.*, 37) was obtained. This result is rationalized in terms of an inefficient interaction between the ligand and CatB, in particular relating to the non-interaction of C*l*(vinyl) with the receptor site.

Conclusions

The crystal structures show that the coordination geometry in each of **1**, **2** and **3** can be described as a distorted Ψ-pentagonal bipyramid with two halogens occupying the axial positions and the stereochemically active lone pair of electrons together with a weakly associated halogen and Te···π interaction in **1**, and two weakly associated halogens in **2** and **3**, defining the pentagonal plane. Similarly, in the docked complexes the Te atom is within a distorted Ψ-pentagonal bipyramidal geometry where one Te-halide bond in the original structures of **1**-**4** is replaced by a Te–S_{Cys29} bond. The configuration about the vinyl C=C bond in the crystal structure of (**1**), *i.e.*, *E* changes to *Z* in the docking calculations for (**1'**).

The binding mode of each of (**1'**)-(**4'**) is very similar, fitting efficiently in the active site via the formation of a Te–S_{Cys29} bond and being held in place by a combination of N–H···π, C–H···π, and Cl_{vinyl}···H interactions, spanning the S1, S2, S1' and S2' sub-sites. Thus, it can be expected that species derived from **1**-**3** will display similar inhibition behavior to the proven species derived from (**4**).[17] In order to ascertain whether the groups bound to the Te atom are significant for the inhibition of cathepsin B, further studies are being performed with molecules presenting different substituent patterns.

Supplementary Information

Supplementary data are available free of charge at http://jbcs.sbq.org.br, as a PDF file.

Acknowledgements

We thank the Brazilian Agencies FAPESP (07/59404-2 to H. A. S.), CNPq (300613/2007 to H. A. S., 306532/2009-3 to J. Z.-S., 140925/2009-0 to S. H. M.) and CAPES (Rede Nanobiotec-Brasil 808/2009 to J. Z.-S. and I. C.) for financial support.

References

1. Zukerman-Schpector, J.; Haiduc, I.; *Phosphorus, Sulfur Silicon Relat. Elem.* **2001,** *171*, 73.
2. Haiduc, I.; Zukerman-Schpector, J.; *Phosphorus, Sulfur Silicon Relat. Elem.* **2001,** *171*, 171.
3. Zukerman-Schpector, J.; Haiduc, I.; *CrystEngComm* **2002**, *33*, 178.
4. Tiekink, E. R. T.; Zukerman-Schpector, J.; *CrystEngComm* **2009,** *11*, 2701.
5. Tiekink, E. R. T.; Zukerman-Schpector, J.; *Coord. Chem. Rev.* **2010,** *254*, 46.
6. Sredni, B.; Caspi, R. R.; Klein, A.; Kalechman, Y.; Danziger, Y.; Benyaakov, M.; Tamari, T.; Shalit, F.; Albeck, M.; *Nature* **1987,** *330*, 173.
7. Albeck, A.; Weitman, H.; Sredni, B.; Albeck, M.; *Inorg. Chem.* **1998,** *37*, 1704.
8. Brodsky, M.; Yosef, S.; Galit, R.; Albeck, M.; Longo, D. L.; Albeck, A.; Sredni, B.; *J. Interferon Cytokine Res.* **2007,** *27*, 453.
9. Sredni, B.; Gal, R.; Cohen, I. J.; Dazard, J. E.; Givol, D.; Gafter, U.; Motro, B.; Eliyahu, S.; Albeck, M.; Lander, H. M.; Kalechman, Y.; *FASEB J.* **2004,** *18*, 400.
10. Yosef, S.; Brodsky, M.; Sredni, B.; Albeck, A.; Albeck, M.; *ChemMedChem* **2007,** *2*, 1601; Brodsky, M.; Hirsh, S.; Albeck, M.; Sredni, B.; *J. Hepatology* **2009,** *51,* 491.
11. Brodsky, M.; Halpert, G.; Albeck, M.; Sredni, B.; *J. Inflammation-London* **2010,** *7:3*.
12. Kenig, S.; Alonso, M. B. D.; Mueller, M. M.; Lah, T. T.; *Cancer Lett.* **2010,** *289*, 53, and references therein.
13. Haque, A.; Banik, N. L.; Ray, S. K.; *CNS Neurol. Disord.: Drug Targets* **2008,** *7*, 270.
14. Homma, A.; Sato, H.; Tamura, T.; Okamachi, A.; Emura, T.; Ishizawa, T.; Kato, T.; Matsuura, T.; Sato, S.; Higuchi, Y.; Watanabe, T.; Kitamura, H.; Asanuma, K.; Yamazaki, T.; Ikemi, M.; Kitagawa, H.; Morikawa, T.; Ikeya, H.; Maeda, K.; Takahashi, K.; Nohmi, K.; Izutani, N.; Kanda, M.; Suzuki, R.; *Bioorg. Med. Chem.* **2010,** *18*, 1062.
15. Lecaille, F.; Kaleta, J.; Brömme, D.; *Chem. Rev.* **2002,** *102*, 4459.
16. Cunha, R. L. O. R.; Urano, M. E.; Chagas, J. R.; Almeida, P. C.; Bincoletto, C.; Tersariol, I. L. S.; Comasseto, J. V.; *Bioorg. Med. Chem. Lett.* **2005,** *15*, 755.
17. Cunha, R. L. O. R.; Gouvea, I. E.; Feitosa, G. P. V.; Alves, M. F. M.; Brömme, D.; Comasseto, J. V.; Tersariol, I. L. S.; Juliano, L.; *Biol. Chem.* **2009,** *390*, 1205.
18. Cunha, R. L. O. R.; Zukerman-Schpector, J.; Caracelli, I.; Comasseto, J. V.; *J. Organomet. Chem.* **2006**, *691*, 4807.

19. Zukerman-Schpector, J.; Comasseto, J. V.; Stefani, H. A.; *Acta Crystallogr., Sect. C: Cryst. Struct. Commun.* **1995**, *51*, 861; Allen, F. H.; *Acta Crystallogr., Sect. B: Struct. Sci.* **2002**, *58*, 380; Allen, F. H., Motherwell, W. D. S.; *Acta Crystallogr., Sect. B: Struct. Sci.* **2002**, *58*, 407.
20. Moura Campos, M.; Petragnani, N.; *Tetrahedron* **1962**, *18* , 527; Uemura, S.; Miyoshi, H.; Okano, M.; *Chem. Lett.* **1979**, *11*, 1357; Comasseto, J. V.; Stefani, H. A.; Chieffi, A.; Zukerman-Schpector, J.; *Organometallics* **1991**, *10*, 845; Zeni, G.; Chieffi, A.; Cunha, R.; Zukerman-Schpector, J.; Stefani, H. A.; Comasseto, J. V.; *Organometallics* **1999,** *18*, 803; Guadagnin, R. C.; Suganuma, C. A.; Singh, F. V.; Vieira, A. S.; Cella, R.; Stefani, H. A.; *Tetrahedron Lett.* **2008**, *49*, 4713.
21. Altomare, A.; Burla, M. C.; Camalli, M.; Cascarano, G. L.; Giacovazzo, C.; Guagliardi, A.; Moliterni, A. G. G.; Polidori, G.; Spagna, R.; *J. Appl. Crystallogr.* **1999**, *32*, 115.
22. Sheldrick, G. M.; *Acta Crystallogr. A* **2008**, *64*, 112.
23. Nardelli, M.; *J. Appl. Crystallogr*. **1995**, *28,* 659.
24. Spek, A. L.; *J. Appl. Crystallogr.* **2003**, *36*, 7.
25. Farrugia, L. J.; *J. Appl. Crystallogr.* **1999,** *32*, 837.
26. Farrugia, L. J.; *J. Appl. Crystallogr.* **1997**, *30*,565.
27. ChemAxon, Marvin 5.1.4 (http://www.chemaxon.com) 2008.
28. Brandenburg, K.; DIAMOND, Crystal Impact GbR, Bonn, Germany, 2006.
29. *GOLD*, version 4.1.1; Cambridge Crystallographic Data Centre: Cambrigde, U.K.; http://www.ccdc.cam.ac.uk/products/life_sciences/gold/; Jones, G.; Willett, P.; Glen, R. C.; *J. Mol. Biol.* **1995,** *245*, 43.
30. Jones, G.; Willett, P.; Glen, R. C.; Leach, A. R.; Taylor, R.; *J. Mol. Biol.* **1997,** *267*, 727.
31. Greenspan, P. D.; Clark, K. L.; Tommasi, R. A.; Cowen, S. D.; McQuire, L. W.; Farley, D. L.; van Duzer, J. H.; Goldberg, R. L.; Zhou, H. H.; Du, Z. M.; Fitt, J. J.; Coppa, D. E.; Fang, Z.; Macchia, W.; Zhu, L. J.; Capparelli, M. P.; Goldstein, R.; Wigg, A. M.; Doughty, J. R.; Bohacek, R. S.; Knap, A. K.; *J. Med. Chem.* **2001,** *44*, 4524.
32. PDB: http://www.rcsb.org/pdb/home/home.do; PDBSum: http://www.ebi.ac.uk/pdbsum/
33. Accelrys DS Visualizer v2.0.1.7347 (http://accelrys.com/)
34. Mooibroek, T. J.; Gamez, P.; Reedijk, J.; *CrystEngComm* **2008**, *10,* 1501.
35. Tiekink, E. R. T.; Zukerman-Schpector, J.; *CrystEngComm* **2009**, *11*, 1176.
36. Tiekink, E. R. T.; Zukerman-Schpector, J.; *Aust. J. Chem.* **2010**, *63*, 535.
37. Zukerman-Schpector, J.; Stefani, H. A.; Guadagnin, R. C.; Suganuma, C. A.; Tiekink, E. R. T.; *Z. Kristallogr.* **2008,** *223*, 536.
38. Zukerman-Schpector, J.; Castellano, E. E.; Oliva, G.; Comasseto, J. V.; Stefani, H. A.; *Acta Crystallogr., Sect. C: Cryst. Struct. Commun.* **1991,** *47*, 960.
39. Kuan, F. S.; Ho, S. Y.; Tadbuppa, P. P.; Tiekink, E. R. T.; *CrystEngComm* **2008,** *10*, 548.
40. Teijido, M.V.; Zukerman-Schpector, J.; Camillo, R. L.; Caracelli, I.; Stefani, H. A.; Chieffi, A.; Comasseto, J. V.; *Z. Kristallogr.* **2003,** *218***,** 636.
41. Zukerman-Schpector, J.; Haiduc, I.; Dabdoub, M. J.; Biazzotto, J. C.; Braga, A. L.; Dornelles, L.; Caracelli, I.; *Z. Kristallogr*. **2002**, *217*, 609.
42. Zukerman-Schpector, J.; Haiduc, I.; Camillo, R. L.; Comasseto, J. V.; Cunha, R. L. O. R.; Caracelli, I.; *Acta Crystallogr.,C* **2001**, *57*,749.
43. Meyers, E. A.; Zingaro, R. A.; Comasseto, J. V.; Stefani, H. A.; *Z. Kristallogr***. 1995**, *210*, 306.
44. Zukerman-Schpector, J.; Haiduc, I.; Dabdoub, M. J.; Biazzotto, J. C.; Braga, A. L.; Dornelles, L.; Caracelli, I.; *Z. Kristallogr.* **2002**, *217*,609.
45. Zukerman-Schpector, J.; Stefani, H. A.; Silva, D. D. O.; Braga, A. L.; Dornelles, L.; Silveira, C. DaC.; Caracelli, I.; *Acta Crystallogr. C* **1998**, *54*,2007.
46. Lu, W.-M.; Wang, Y.-P.; Huang, X.; Sun, J.; *Chin. J. Chem.* **2001**, *19*, 457.
47. Buntine, M. A.; Hall, V. J.; Kosovel, F. J.; Tiekink, E. R. T.; *J. Phys. Chem. A* **1998,** *102*, 2472.
48. Schechter, I.; Berger, A.; *Biochem. Biophys. Res. Commun.* **1967,** *27*, 157
49. Watanabe, D.; Yamamoto, A.; Tomoo, K.; Matsumoto, K.; Murata, M.; Kitamura, K.; Ishida, T.; *J. Mol. Biol.* **2006,** *362*, 979.

Submitted: June 7, 2010
Published online: August 17, 2010

FAPESP has sponsored the publication of this article.

J. Braz. Chem. Soc., Vol. 00, No. 00, S1-S3, 2010.
Printed in Brazil - ©2010 Sociedade Brasileira de Química
0103 - 5053 $6.00+0.00

2-Chlorovinyl Tellurium Dihalides, (*p*-tol)Te[C(H)=C(C*l*)Ph]X_2 for X = C*l*, Br and I: Variable Coordination Environments, Supramolecular Structures and Docking Studies in Cathepsin B

Ignez Caracelli,*,[a] Julio Zukerman-Schpector,*,[b] Stella H. Maganhi,[b] Hélio A. Stefani,[c] Rafael Guadagnin[d] and Edward R. T. Tiekink*,[e]

[a]*Departamento de Física, Universidade Federal de São Carlos, CP 676, 13565-905 São Carlos-SP, Brazil*

[b]*Laboratório de Cristalografia, Estereodinâmica e Modelagem Molecular, Departamento de Química, Universidade Federal de São Carlos, CP 676, 13565-905 São Carlos-SP, Brazil*

[c]*Departamento de Farmácia, Faculdade de Ciências Farmacêuticas, Universidade de São Paulo, São Paulo-SP, Brazil*

[d]*Departamento de Química, Universidade Federal de São Paulo, São Paulo-SP, Brazil*

[e]*Department of Chemistry, University of Malaya, 50603 Kuala Lumpur, Malaysia*

Table S1. Complete set of data interactions

subsite	S1	S1'	S2	S2'

TeI interactions				
TeI GOLDScore: 44.97 kcal mol^{-1} $\Delta G_{binding}$: –7.10 kcal mol^{-1}				
Subsite	TeI···cathepsin interaction	distance (Å)	TeI ligand atom	1gmy atom
S2'	I2 - GLU122:OE2	3.32	I2	OE2
	C*l*3 - GLN23:HE21	2.86	**Cl3**	HE21
S1'	Te1 - GLY27:O	2.91	Te1	O
	C*l*3 - GLY27:HA1	3.24	**Cl3**	HA1
	C*l*3 - GLY27:HA2	2.44	**Cl3**	HA2
	H5 - MET196:O	3.10	H5	O
	H5 - GLY197:O	2.32	H5	O
S1	I2 - ASN72:O	3.18	I2	O
	I2 - GLY73:HA1	3.13	I2	HA1
	I2 - GLY73:HA2	3.43	I2	HA2
	Te1 - CYS29:SG	**2.971**	**Te1**	**SG**
	Te1 - GLY73:HA2	2.93	Te1	HA2
	H13 - GLY74:O	2.34	H13	O
	H15B - GLY74:O	3.14	H15B	O
S2	H1 - GLY198:O	2.48	H1	O
	H4 - GLY198:O	2.52	H4	O

*e-mail: ignez@ufscar.br, julio@power.ufscar.br, edward.tiekink@gmail.com

TeC*l* interactions

TeC*l* GOLDScore: 45.55 kcal mol^{-1}
$\Delta G_{binding}$: −7.16 kcal mol^{-1}

Subsite	TeC*l*···cathepsin interaction	distance (Å)	TeCl ligand atom	1gmy atom
S2'	C*l*3 - GLN23:HE21	2.66	**Cl3**	HE21
S1'	Te1 - GLY27:O	3.43	Te1	O
	C*l*3 - GLY27:HA2	2.91	**Cl3**	HA2
	H7 - MET196:O	2.56	H7	O
	H7 - GLY197:O	2.74	H7	O
	H8 - MET196:O	3.37	H8	O
	H8 - GLY197:O	3.26	H8	O
S1	Te1 - CYS29:SG	3.21	Te1	SG
	C*l*2 - ASN72:O	3.22	Cl2	O
	C*l*2 - GLY73:HA1	2.40	Cl2	HA1
	C*l*2 - GLY73:HA2	3.03	Cl2	HA2
	H11 - GLY74:O	3.35	H11	O
S2	C*l*3 - HIS199:HD1	2.87	Cl3	HD1
	H1 - GLY198:O	2.16	H1	O
	H4 - HIS199:ND1	3.04	H4	ND1
	H8 - GLY198:O	2.95	H8	O
	H13 - GLY198:O	3.20	H13	O
	H14 - GLY198:O	2.44	H14	O

TeBr interactions

TeBr GOLDScore: 43.09 kcal mol^{-1}
$\Delta G_{binding}$: −6.90 kcal mol^{-1}

Subsite	TeBr···cathepsin interaction	distance (Å)	TeBr ligand atom	1gmy atom
S2'	C*l*3 - GLN23:HE21	3.39	**Cl3**	HE21
	C*l*3 - GLU122:OE2	3.45	**Cl3**	OE2
S1'	Te - GLY27:O	3.21	Te	O
	C*l*3 - GLY27:HA1	2.86	**Cl3**	HA1
	C*l*3 - GLY27:HA2	2.48	**Cl3**	HA2
	H4 - GLY197:O	3.43	H4	O
	H5 - MET196:O	3.01	H5	O
	H5 - GLY197:O	2.58	H5	O
S1	Te - CYS29:SG	2.90	Te	SG
	Br2 - ASN72:O	3.43	Br2	O
	Br2 - GLY73:HA1	2.69	Br2	HA1
	Br2 - GLY73:HA2	3.15	Br2	HA2
	H13 - GLY74:O	3.32	H13	O
S2	H1 - GLY198:O	2.22	H1	O
	H4 - GLY198:O	2.66	H4	O
	H10 - GLY198:O	2.35	H10	O
	H11 - GLY198:O	3.19	H11	O

YOWMEC interactions				
YOWMEC GOLDScore: 42.79 kcal mol^{-1} $\Delta G_{binding}$: –6.87 kcal mol^{-1}				
Subsite	YOWMEC–cathepsin interaction	distance (Å)	YOWMEC ligand atom	1gmy Atom
S2'	C*l*3 - GLN23:HE21	2.93	**Cl3**	HE21
S1'	Te1 - GLY27:O	3.21	Te1	O
	C*l*3 - GLY27:HA1	3.33	**Cl3**	HA1
	C*l*3 - GLY27:HA2	2.56	**Cl3**	HA2
	H5 - MET196:O	2.98	H5	O
	H5 - GLY197:N	2.79	H5	N
	H5 - GLY197:O	2.58	H5	O
	H6 - GLY197:O	3.41	H6	O
S1	Te1 - CYS29:SG	2.90	Te1	SG
	H1 - CYS29:SG	2.98	H1	SG
	H9 - GLY74:O	2.79	H9	O
	H10 - CYS29:SG	2.59	H10	SG
	H12 - GLY74:O	2.90	H12	O
S2	H1 - GLY198:O	2.41	H1	O
	H6 - GLY198:O	2.70	H6	O
	H7 - GLY198:O	2.33	H7	O
	H8 - GLY198:N	3.42	H8	N
	H8 - GLY198:O	2.87	H8	O